Zero-sequence current control of modular active power filter for high power three-phase three-wire electrical networks

Mohamed Choukri Benhabib, Philippe Poure, Shahrokh Saadate

Zero-sequence current control of Modular Active Power Filter for high power three-phase three-wire electrical networks

M. C. Benhabib*, P. Poure** and S. Saadate*

** Groupe de Recherche en Electrotechnique et Electronique de Nancy, GREEN-UHP CNRS UMR 7037*

Université Henri Poincaré Nancy 1, B.P. 239, 54506 Vandoeuvre lès Nancy, France

Email address: bmchouk@caramail.com and shahrokh.Saadate@green.uhp-nancy.fr

*** Laboratoire d'Instrumentation Electronique de Nancy LIEN – UHP*

Faculté des Sciences et Techniques – BP 239 – 54506 Vandoeuvre les Nancy cedex France

Email address: philippe.poure@lien.uhp-nancy.fr

Abstract

Since the development of the first control strategy for the active power filters (APF) introduced by H. Akagi [H. Akagi, Y. Kanazawa,A. Nabae, Generalized theory of the instantaneous reactive power in three-phase circuits, in: Proceedings of International Power Electronics Conference, Tokyo, Japan (1983) 1375–1386.], many efforts have been concentrated to improve their performances. However, when electrical networks supplies high current non-linear loads, a single inverter-based APF has limited power capability. In this paper, we studied parallel operation achieving high power level. More particularly, we examined a modular APF based on two three-phase inverters. This structure allows zero-sequence current circulating through the inverters, as demonstrated by using averaged modelling of the APF. To solve this problem and based on previous averaged model, we proposed a new optimal control strategy, suppressing the zero-sequence circulating current. Simulation results validate the proposed control.

Keywords: Modular Active Power Filter (APF); parallel operation; zero-sequence current; instantaneous power theory; averaged modelling.

1. Introduction

In the last two decades development of many control strategies for Active Power Filters (APF's) has been performed. Most of them concern control methods based on the instantaneous powers, introduced by Akagi [1]. Other control strategies performed filtering in three-wire and four-wire electrical networks [2-6].

However, when electrical network supplies high current non-linear loads, a single inverter used as APF always has limited power capability, due to the fundamental limitations of semiconductor devices. For example, Insulated Gate Bipolar Transistors (IGBT), are current limited whereas Gate Turn off components (GTO) have low switching frequency.

To solve this problem, one way to achieve a high power level is to use parallel operation. We present figure 1 a so called " modular " APF using N inverters.

Parallel inverters have the unique advantage of virtually unlimited output power for the APF. In practice, any number of parallel inverters can be chosen, according to the specific power requirements encountered.

More, parallel multi-inverter provides redundancy and allows filtering in low-voltage distribution bus and high-current non-linear loads.

While paralleling is becoming popular, most parallel applications deal with three-phase buck or boost rectifiers [7,8]. But, this was not a common practice because of interactions that cause additional overhead requirements for isolation, such as transformers [8]. Recent studies proposed direct parallel three-phase converter structure [9].

As far as APF is concerned, quad series voltage source pulse width modulated converters have been proposed by Akagi [10]. This structure uses four three-phase transformers for quad-series connection, causing additional overhead requirements [11].

In this paper, we propose a general APF structure based on a modular parallel system where individual inverters connect both DC and AC sides directly without additional requirement.

The proposed study deals with a modular APF for high power three-phase three-wire electrical networks and based on two parallel non isolated inverters. More APF control achieves zero-sequence current suppression.

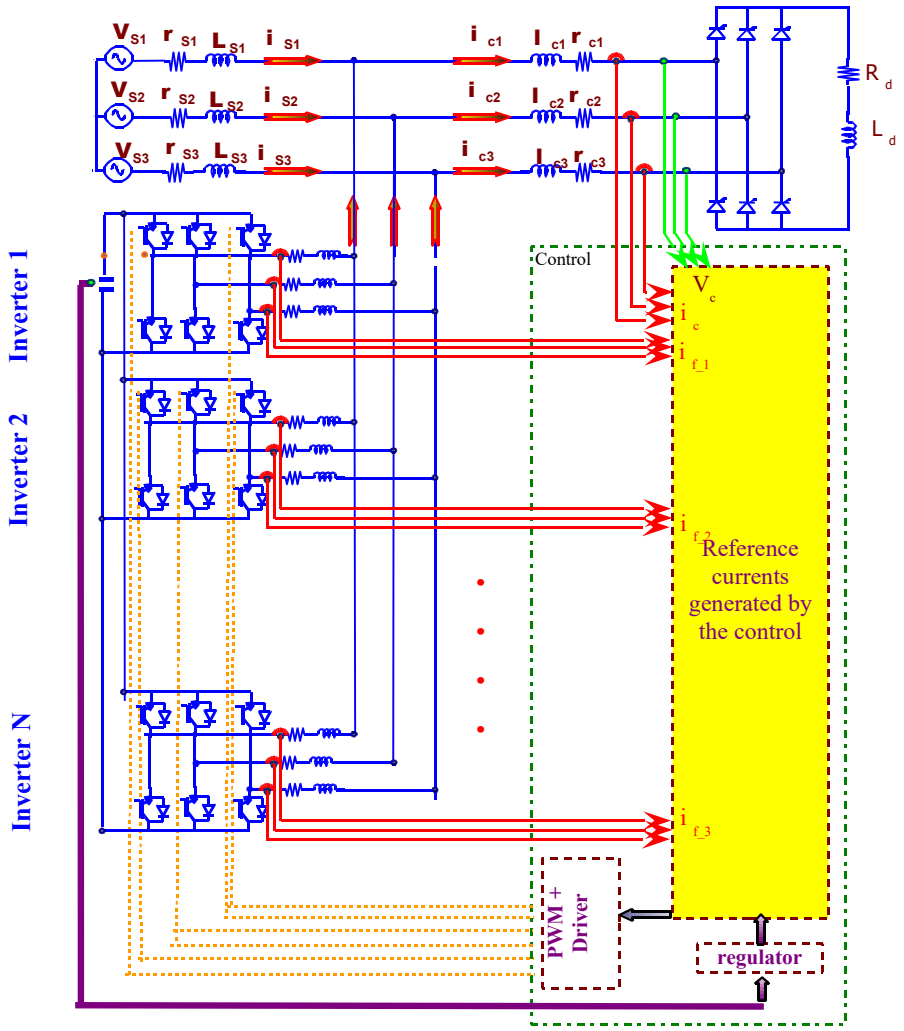

Fig. 1. Modular APF based on parallel structure

In section 2, converter topology is presented and its averaged model developed. An averaged model of the zero-sequence current, circulating through the two inverters, concludes this section.

Based on the previous zero-sequence current model, section 3 proposes an advanced control for both inverters, when using direct control method for the APF. This zero-sequence current control is designed to suppress the zero-sequence circulating current.

Section 4 shows some simulation results and, by this way, validates the developed averaged model and the proposed control.

Conclusion summarizes major contribution of this work and discusses ideas for future work.

2. Averaged Modelling

2.1 APF Topology

In this paper, we study the topology presented (Fig.2). It consists on two parallel three-phase current bidirectional switch based PWM inverters. The AC sides of both inverters are directly connected to the electrical network via inductors as classical APFs. Network internal resistances are modelled (Fig.2). The DC sides of both converters are connected to a single capacitor. Each inverter is based on six switching cells having inherently anti-parallel diodes (IGBTs for example) or external anti-parallel diodes (GTOs associated with anti-parallel diodes).

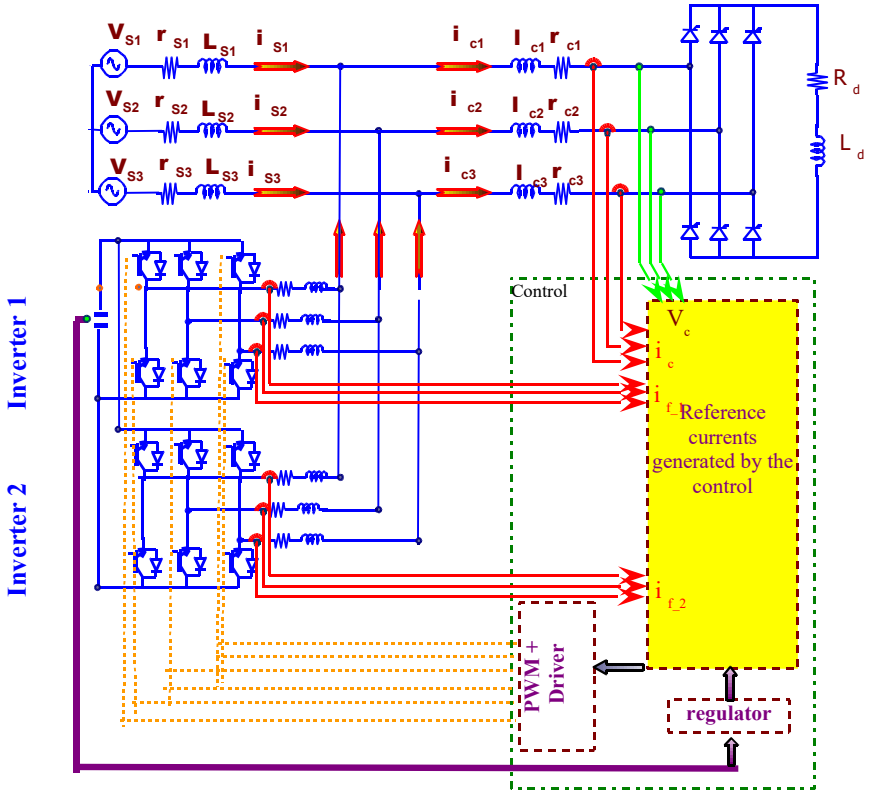

Fig. 2. Modular APF based on two three-phase inverters.

2.2 Averaged modelling in stationary coordinates

Conventionally, the averaging in three-phase current bidirectional inverter is based on line-to-line feature, common-mode components having generally no interest when designing control of a single converter [12].

However, as far as parallel inverters design is concerned, common-mode components are critical. Phase-leg averaged modelling allows to preserve common-mode components [9].

A generic phase-leg is represented (Fig.3), for the phase k where k={a, b, c}. We chose the negative side of v_{dc} as a reference point (see Fig.3).

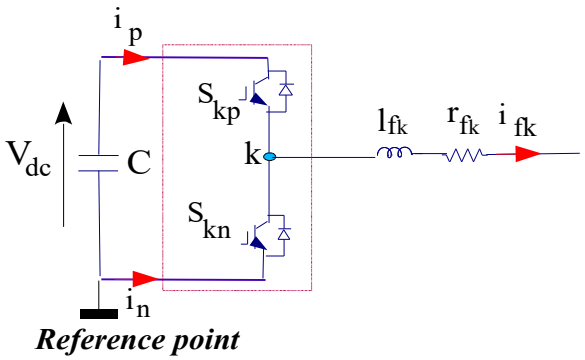

Fig. 3. Generic phase-leg of bidirectional inverter.

Switching constraints on the capacitor C which should not be short-circuited and on the inductor which should not be open circuited result in a complementary switching control of the top S_{kp} and bottom S_{kn} switches as:

$$S_{kp}+S_{kn}=1 \tag{1}$$

Consequently, each generic phase-leg can be modelled by a double-throw switch, depicted below (Fig.4).

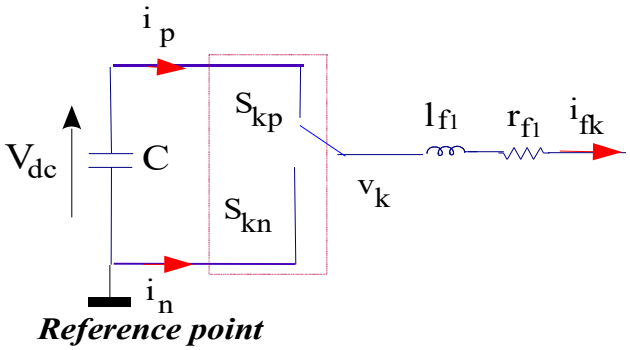

Fig. 4. Double-throw switch model of the phase-leg.

Each double-throw switch as a current source l_{fk} connected to the electrical networks and a voltage source connected to the DC side (capacitor C).

Consequently, both current i_{fk} and voltage v_{dc} can be assumed as continuous.

Based on average modelling over each switching cycle, we obtained the following relations for mean variables:

$$\begin{cases} V_k = d_k V_{dc} \\ I_p = d_k I_{fk} \end{cases} \quad (2)$$

Where d_k is defined as the duty cycle of the top switch S_{kp} on the considered switching cycle. The upper case symbols represent averaged variables whereas the lower case symbols represent instantaneous variables.
The resulting electrical averaged model is given below (Fig.5).

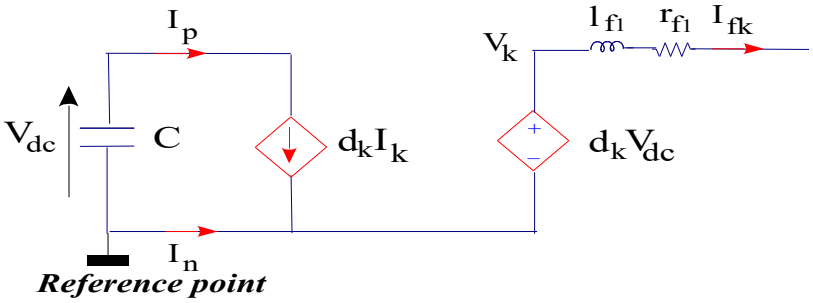

Fig. 5. Averaged model of the k phase-leg.

Based on this model (Fig.5), we obtained (Fig.7) the averaged model of the modular APF with two three-phase inverters (respectively A and B) as presented below (Fig.6).

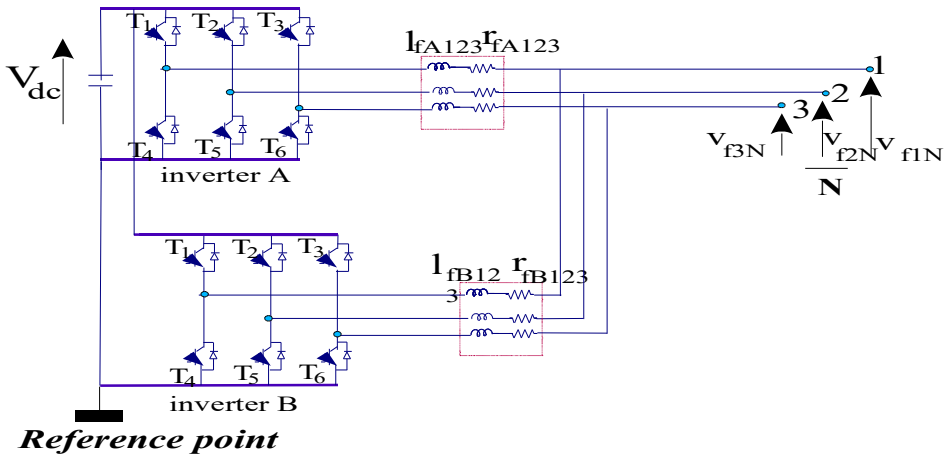

Fig. 6. APF based on two inverters.

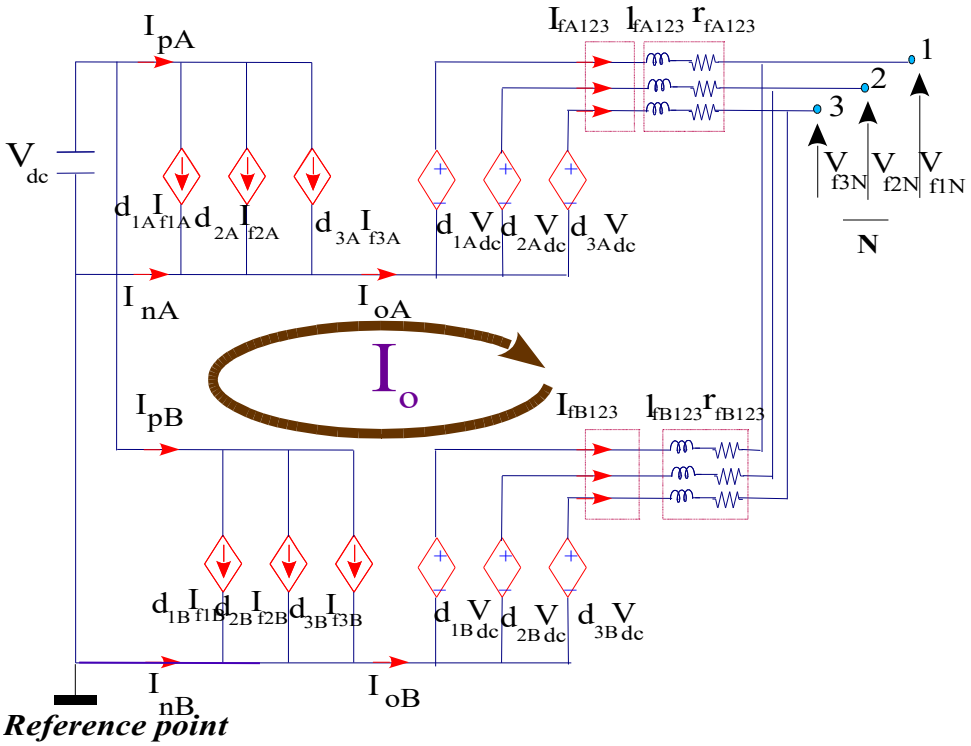

Fig. 7. Averaged model in stationary coordinates with zero-sequence components.

Consequently, when neglecting r_{fk} resistor, the state-space equations of the APF (Fig.7) are the following in stationary coordinates for each of the two inverters A and B :

$$l_{fa}\frac{d}{dt}\begin{bmatrix} I_{fA1} \\ I_{fA2} \\ I_{fA3} \end{bmatrix} = \begin{bmatrix} d_{1A} \\ d_{2A} \\ d_{3A} \end{bmatrix} V_{dc} - \begin{bmatrix} V_{f1N} \\ V_{f2N} \\ V_{f3N} \end{bmatrix} - \begin{bmatrix} V_N \\ V_N \\ V_N \end{bmatrix} \tag{3}$$

$$l_{fB}\frac{d}{dt}\begin{bmatrix} I_{fB1} \\ I_{fB2} \\ I_{fB3} \end{bmatrix} = \begin{bmatrix} d_{1B} \\ d_{2B} \\ d_{3B} \end{bmatrix} V_{dc} - \begin{bmatrix} V_{f1N} \\ V_{f2N} \\ V_{f3N} \end{bmatrix} - \begin{bmatrix} V_N \\ V_N \\ V_N \end{bmatrix} \tag{4}$$

$$\frac{dV_{dc}}{dt} = \frac{1}{C}\left(\begin{bmatrix} d_{1A} & d_{2A} & d_{3A} \end{bmatrix}\begin{bmatrix} I_{1A} \\ I_{2A} \\ I_{3A} \end{bmatrix}\right) + \frac{1}{C}\left(\begin{bmatrix} d_{1B} & d_{2B} & d_{3B} \end{bmatrix}\begin{bmatrix} I_{1B} \\ I_{2B} \\ I_{3B} \end{bmatrix}\right) \quad (5)$$

For a single inverter-based APF the sum of the output filter currents I_{f1A}, I_{f2A} and I_{f3A} has to be null because there is no physical path for zero-sequence current. However, with two parallel inverters, a zero-sequence current path exists physically, as shown (Fig.7). The zero-sequence current I_o is defined by :

$$I_o = I_{oA} = -I_{oB} = d_{1A} I_{f1A} + d_{2A} I_{f2A} + d_{3A} I_{f3A} \quad (6)$$

or

$$I_o = I_{oA} = -I_{oB} = -d_{1B} I_{f1B} - d_{2B} I_{f2B} - d_{3B} I_{f3B} \quad (7)$$

2.3 Averaged modelling in rotating coordinates

Usually, the averaged model in the stationary coordinates is transformed into rotating coordinates [7] when classical boost rectifier, buck rectifier or inverter is studied.

The classical transformation orthogonal matrix T is :

$$T = \sqrt{\frac{2}{3}}\begin{bmatrix} \cos\omega t & \cos\left(\omega t - 2\frac{\pi}{3}\right) & \cos\left(\omega t + 2\frac{\pi}{3}\right) \\ -\sin\omega t & -\sin\left(\omega t - 2\frac{\pi}{3}\right) & -\sin\left(\omega t + 2\frac{\pi}{3}\right) \\ \frac{1}{\sqrt{2}} & \frac{1}{\sqrt{2}} & \frac{1}{\sqrt{2}} \end{bmatrix} \quad (8)$$

Where ω is chosen as the same frequency as the AC electrical networks frequency.

Using the matrix T, we note :

$$\begin{bmatrix} I_{dA} \\ I_{qA} \\ I_{oA} \end{bmatrix} = T\begin{bmatrix} I_{f1A} \\ I_{f2A} \\ I_{f3A} \end{bmatrix} \quad (9)$$

$$\begin{bmatrix} I_{dB} \\ I_{qB} \\ I_{oB} \end{bmatrix} = T \begin{bmatrix} I_{f1B} \\ I_{f2B} \\ I_{f3B} \end{bmatrix} \tag{10}$$

$$\begin{bmatrix} V_{fd} \\ V_{fq} \\ V_{fo} \end{bmatrix} = T \begin{bmatrix} V_{f1N} \\ V_{f2N} \\ V_{f3N} \end{bmatrix} \tag{11}$$

$$\begin{bmatrix} d_{dA} \\ d_{qA} \\ d_{oA} \end{bmatrix} = T \begin{bmatrix} d_{1A} \\ d_{2A} \\ d_{3A} \end{bmatrix} \tag{12}$$

$$\begin{bmatrix} d_{dB} \\ d_{qB} \\ d_{oB} \end{bmatrix} = T \begin{bmatrix} d_{1B} \\ d_{2B} \\ d_{3B} \end{bmatrix} \tag{13}$$

By transforming equations (3) to (5) in the rotating coordinates using matrix T, we obtain :

$$l_{fA} \frac{d}{dt} \begin{bmatrix} I_{dA} \\ I_{qA} \\ I_{oA} \end{bmatrix} = \begin{bmatrix} d_{dA} \\ d_{qA} \\ d_{oA} \end{bmatrix} V_{dc} - l_{fA} \begin{bmatrix} 0 & -\omega & 0 \\ \omega & 0 & 0 \\ 0 & 0 & 0 \end{bmatrix} \begin{bmatrix} I_{dA} \\ I_{qA} \\ I_{oA} \end{bmatrix} - \begin{bmatrix} V_{fd} \\ V_{fq} \\ V_{fo} \end{bmatrix} - \begin{bmatrix} 0 \\ 0 \\ \sqrt{3} V_N \end{bmatrix} \tag{14}$$

$$l_{fB} \frac{d}{dt} \begin{bmatrix} I_{dB} \\ I_{qB} \\ I_{oB} \end{bmatrix} = \begin{bmatrix} d_{dB} \\ d_{qB} \\ d_{oB} \end{bmatrix} V_{dc} - l_{fB} \begin{bmatrix} 0 & -\omega & 0 \\ \omega & 0 & 0 \\ 0 & 0 & 0 \end{bmatrix} \begin{bmatrix} I_{dB} \\ I_{qB} \\ I_{oB} \end{bmatrix} - \begin{bmatrix} V_{fd} \\ V_{fq} \\ V_{fo} \end{bmatrix} - \begin{bmatrix} 0 \\ 0 \\ \sqrt{3} V_N \end{bmatrix} \tag{15}$$

$$\frac{d V_{dc}}{dt} = \frac{1}{C} \left(\begin{bmatrix} d_{dA} & d_{qA} & \frac{d_{oA}}{\sqrt{3}} \end{bmatrix} \begin{bmatrix} I_{dA} \\ I_{qA} \\ I_{oA} \end{bmatrix} \right) + \frac{1}{C} \left(\begin{bmatrix} d_{dB} & d_{qB} & \frac{d_{oB}}{\sqrt{3}} \end{bmatrix} \begin{bmatrix} I_{dB} \\ I_{qB} \\ I_{oB} \end{bmatrix} \right) \tag{16}$$

By using $I_o = I_{oA} = - I_{oB}$, we obtain:

$$l_{fA} \frac{d}{dt} \begin{bmatrix} I_{dA} \\ I_{qA} \end{bmatrix} = \begin{bmatrix} d_{dA} \\ d_{qA} \end{bmatrix} V_{dc} - l_{fA} \begin{bmatrix} 0 & -\omega \\ -\omega & 0 \end{bmatrix} \begin{bmatrix} I_{dA} \\ I_{qA} \end{bmatrix} - \begin{bmatrix} V_{fd} \\ V_{fq} \end{bmatrix} \tag{17}$$

$$l_{fB}\frac{d}{dt}\begin{bmatrix} I_{dB} \\ I_{qB} \end{bmatrix} = \begin{bmatrix} d_{dB} \\ d_{qB} \end{bmatrix} V_{dc} - l_{fB}\begin{bmatrix} 0 & -\omega \\ \omega & 0 \end{bmatrix}\begin{bmatrix} I_{dB} \\ I_{qB} \end{bmatrix} - \begin{bmatrix} V_{fd} \\ V_{fq} \end{bmatrix} \tag{18}$$

$$\frac{dI_o}{dt} = -\frac{(d_{oA} - d_{oB})V_{dc}}{l_{fA} + l_{fB}} = \frac{-\Delta d_o V_{dc}}{l_{fA} + l_{fB}} \tag{19}$$

$$\frac{d V_{dc}}{dt} = \frac{1}{C}\left(\begin{bmatrix} d_{dA} & d_{qA} \end{bmatrix}\begin{bmatrix} I_{dA} \\ I_{qA} \end{bmatrix} + \begin{bmatrix} d_{dB} & d_{qB} \end{bmatrix}\begin{bmatrix} I_{dB} \\ I_{qB} \end{bmatrix}\right) + \frac{\Delta d_o I_o}{\sqrt{3}} \tag{20}$$

Thus, the final averaged model of the modular active power filter in rotating coordinates is illustrated (Fig. 8).

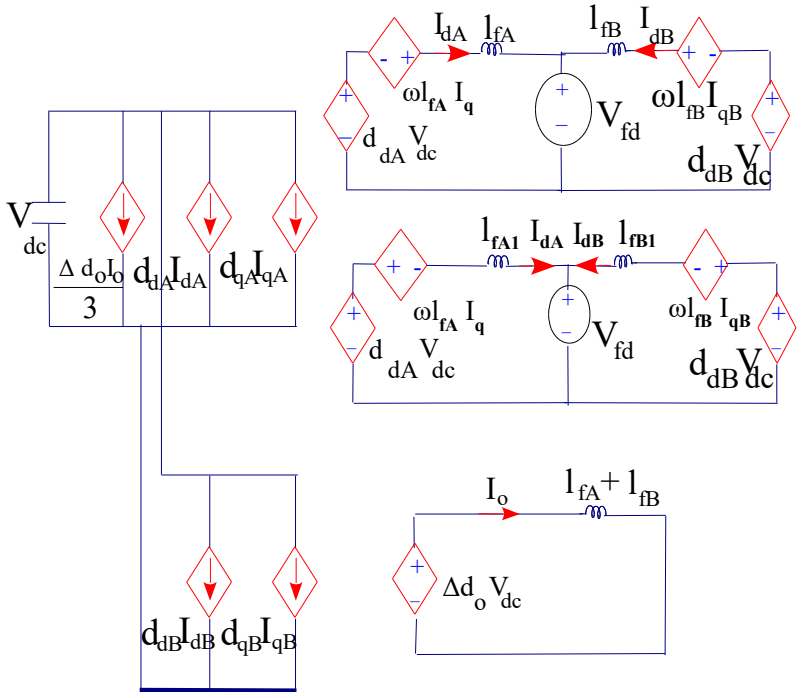

Fig. 8. Averaged model of the modular APF in d-q-o coordinates.

The averaged model of the APF presented (Fig.8) demonstrates that a zero-sequence current circulates between the two inverters. It is defined by Eqs. (19). Consequently, a classical control design for each individual inverter is not well suited for suppressing zero-sequence current in parallel operation. We

propose in the next section a new PWM control concept to suppress this zero-sequence current. This PWM control method is interesting in that it does not need any additional circuit.

3. Control strategy presentation

3.1 Harmonic currents identification

The control method studied in this paper is based on the synchronous reference frame [13].

Namely, we note $i_{c1}(t)$, $i_{c2}(t)$, $i_{c3}(t)$ the line currents of the three-phase three-wire system. The Concordia transformation permits to bring back the balanced three-phase system to two-phase system, by the following expression :

$$\begin{bmatrix} i_\alpha \\ i_\beta \end{bmatrix} = \sqrt{\frac{2}{3}} \begin{bmatrix} 1 & -\frac{1}{2} & -\frac{1}{2} \\ 0 & \frac{\sqrt{3}}{2} & -\frac{\sqrt{3}}{2} \end{bmatrix} \begin{bmatrix} i_{c1} \\ i_{c2} \\ i_{c3} \end{bmatrix} \tag{21}$$

We use a robust Phase Locked Loop (P.L.L) detailed in [14] to generate $\sin(\hat{\theta})$ and $\cos(\hat{\theta})$ signals. We obtain the following equation :

$$\begin{bmatrix} i_d \\ i_q \end{bmatrix} = \begin{bmatrix} \sin(\hat{\theta}) & -\cos(\hat{\theta}) \\ \cos(\hat{\theta}) & \sin(\hat{\theta}) \end{bmatrix} \begin{bmatrix} i_\alpha \\ i_\beta \end{bmatrix} \tag{22}$$

These d-q components can be expressed as the sum of a continuous component and an alternative component :

$$\begin{bmatrix} i_d \\ i_q \end{bmatrix} = \begin{bmatrix} \bar{i}_d + \tilde{i}_d \\ \bar{i}_q + \tilde{i}_q \end{bmatrix} \tag{23}$$

With $\bar{i}_d$ and $\bar{i}_q$ the continuous component of i_d and i_q,
and $\tilde{i}_d$ and $\tilde{i}_q$ the alternative components.

From equation (23), we deduct the current components in the α-β coordinates :

$$\begin{bmatrix} i_\alpha \\ i_\beta \end{bmatrix} = \begin{bmatrix} \sin(\hat{\theta}) & -\cos(\hat{\theta}) \\ \cos(\hat{\theta}) & \sin(\hat{\theta}) \end{bmatrix}^{-1} \begin{bmatrix} i_d \\ i_q \end{bmatrix} = \begin{bmatrix} \sin(\hat{\theta}) & \cos(\hat{\theta}) \\ -\cos(\hat{\theta}) & \sin(\hat{\theta}) \end{bmatrix} \begin{bmatrix} i_d \\ i_q \end{bmatrix} \quad (24)$$

Namely :

$$\begin{bmatrix} i_\alpha \\ i_\beta \end{bmatrix} = \begin{bmatrix} \sin(\hat{\theta}) & \cos(\hat{\theta}) \\ -\cos(\hat{\theta}) & \sin(\hat{\theta}) \end{bmatrix} \begin{bmatrix} \bar{i}_d \\ \bar{i}_q \end{bmatrix} + \begin{bmatrix} \sin(\hat{\theta}) & \cos(\hat{\theta}) \\ -\cos(\hat{\theta}) & \sin(\hat{\theta}) \end{bmatrix} \begin{bmatrix} \tilde{i}_d \\ \tilde{i}_q \end{bmatrix} \quad (25)$$

One can choose compensating harmonic currents and/or reactive power as depicted in table 1.

	Harmonics current compensation	**Reactive energy compensation**	**Harmonics current and reactive energy compensation**
Control parameters	$i_{dc} = \tilde{i}_d$ and $i_{qc} = \tilde{i}_q$	$i_{dc} = 0$ and $i_{qc} = \bar{i}_q$	$i_{dc} = \tilde{i}_d$ and $i_{qc} = i_q$

Table 1. Harmonic currents and/or reactive power compensation.

When compensating harmonic currents and reactive power simultaneously, the Eqs. (25) becomes :

$$\begin{bmatrix} i_{f\alpha}^{ref} \\ i_{f\beta}^{ref} \end{bmatrix} = \begin{bmatrix} \sin(\hat{\theta}) & \cos(\hat{\theta}) \\ -\cos(\hat{\theta}) & \sin(\hat{\theta}) \end{bmatrix} \begin{bmatrix} \tilde{i}_d \\ i_q \end{bmatrix} \quad (26)$$

Then the inverse concordia transformation leads to reference currents :

$$\begin{bmatrix} i_{f1}^{ref} \\ i_{f2}^{ref} \\ i_{f3}^{ref} \end{bmatrix} = \sqrt{\frac{2}{3}} \begin{bmatrix} 1 & 0 \\ -\frac{1}{2} & \frac{\sqrt{3}}{2} \\ -\frac{1}{2} & -\frac{\sqrt{3}}{2} \end{bmatrix} \begin{bmatrix} i_{f\alpha}^{ref} \\ i_{f\beta}^{ref} \end{bmatrix} \quad (27)$$

The following figure illustrates the harmonic currents identification :

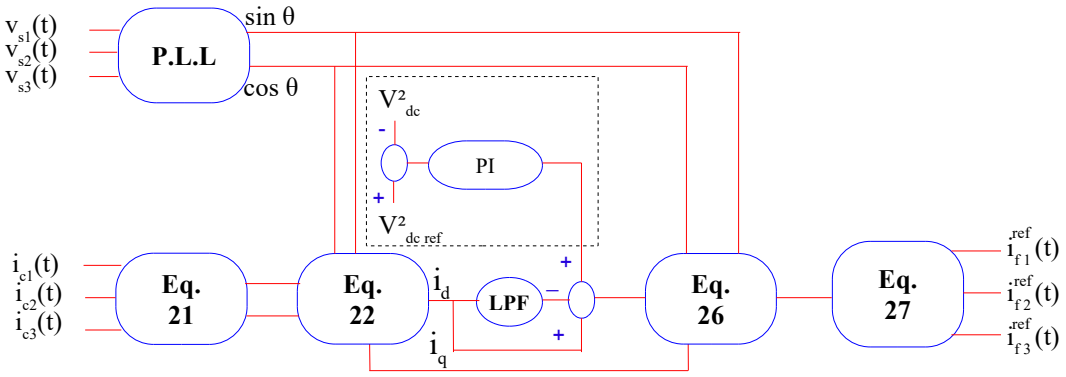

Fig. 11. Synchronous reference frame control for the modular active power filter.

3.2 Zero-sequence current suppression

From Eqs. (19), we can suppress zero-sequence current when :

$$\Delta d_o = d_{oA} - d_{oB} = 0 \quad (28)$$

Eqs. (28) is achieved when the following conditions are verified :

- Harmonic currents references must be the same for inverters A and B,
- PWM triangular signals must be the same for inverters A and B.

Consequently, we propose a PWM control strategy (Fig. 12) when only one triangular signal is used. More, the two harmonic currents references are chosen equal for the two inverters and defined by :

$$
\begin{aligned}
i_{f1A}^{ref} &= i_{f1B}^{ref} = i_{f1}^{ref}/2 \\
i_{f2A}^{ref} &= i_{f2B}^{ref} = i_{f2}^{ref}/2 \\
i_{f3A}^{ref} &= i_{f3B}^{ref} = i_{f3}^{ref}/2
\end{aligned} \tag{29}
$$

Where $i_{f1}^{ref}, i_{f2}^{ref}$ and i_{f3}^{ref} are defined by (27).

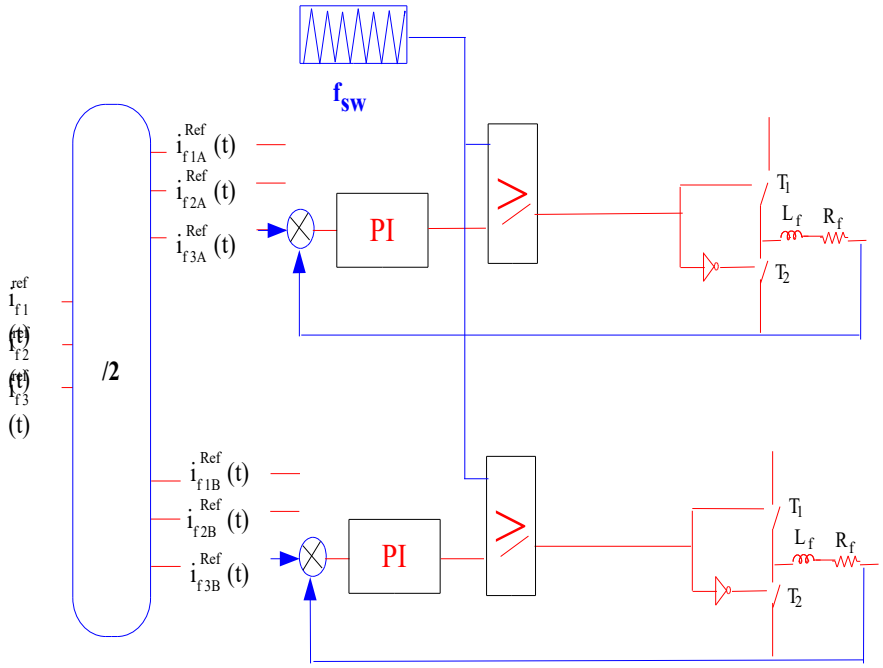

Fig. 12. PWM control strategy.

4. Simulation results

4.1 Zero-sequence current simulation

We simulated a two-inverter based APF with parameters defined in Appendix A when using PWM control strategy (Fig. 12 and 13). In the case (Fig.13) two PWM triangular signals are used for inverters A and B, with f_{swA} and f_{swB} frequencies respectively. The zero-sequence current for this case is given (Fig,14).

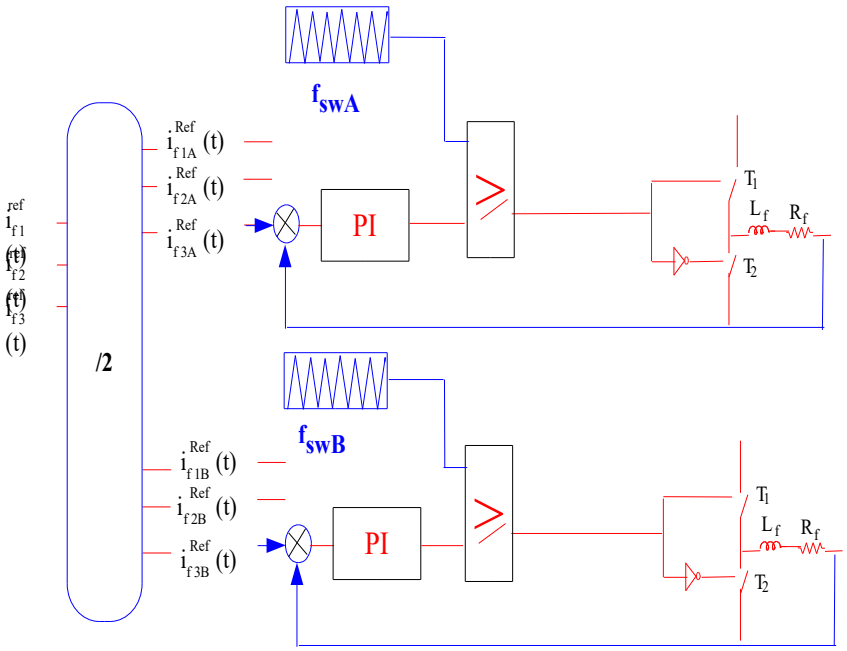

Fig. 13. Classical PWM control strategy with $f_{sw\,A}$ = 5 KHz and $f_{sw\,B}$ = 4,9 KHz.

Following simulations show the elimination of this zero-sequence current (circulating between the two inverters) by using the proposed control strategy.

When using control strategy (Fig.12) with f_{sw} = 5 KHz, zero-sequence current can be considered as suppressed (Fig,15). More, if we increase f_{sw} value in the case of control (Fig.12), we improve zero-sequence current elimination (Fig.16).

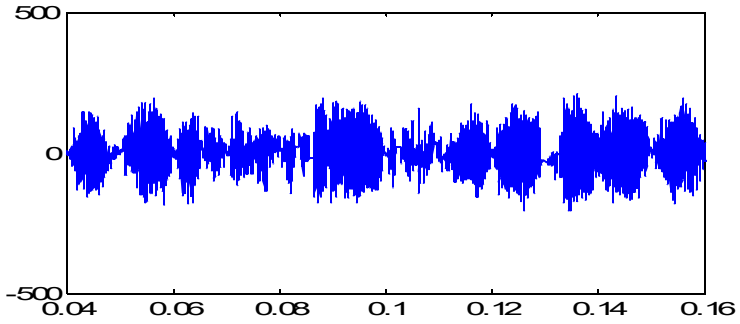

Fig. 14. Zero-sequence current for control (Fig.13)

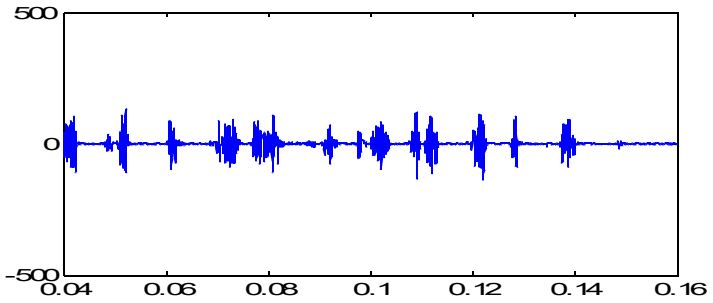

Fig. 15. Zero-sequence current for control (Fig.12) with f_{sw} = 5 KHz

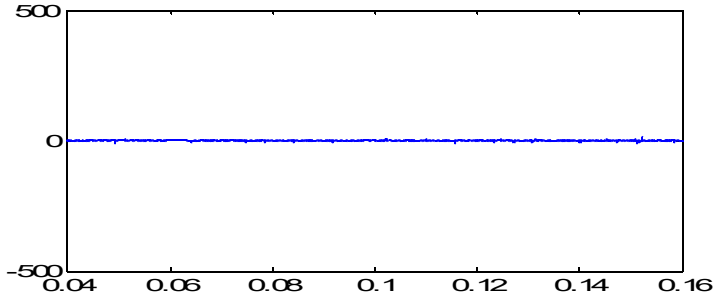

Fig. 16. Zero-sequence current for control (Fig.12) with f_{sw} = 12 KHz

We can note that a zero-sequence current different from zero leads to poor capacitor voltage stabilisation (case Fig.14). Consequently, harmonic currents compensation performances is highly decreased.

In our case, two inverters are used; one could think of using two carriers of opposite signs to improve high frequency ripple in the total output of the APF.

However, such current ripple improvement could not be achieved in general case, but only if an even number of inverters is used.

4.2 Modular APF simulation

We now present general simulation results for a two-inverter based APF, illustrated (Fig.2). The non-linear load is a three-phase thyristor rectifier feeding a (R-L) load. The control angle for the thyristor bridge is 0° from t=0 [sec] to t=0.08 [sec] and becomes 30°at t=0.08 [sec].

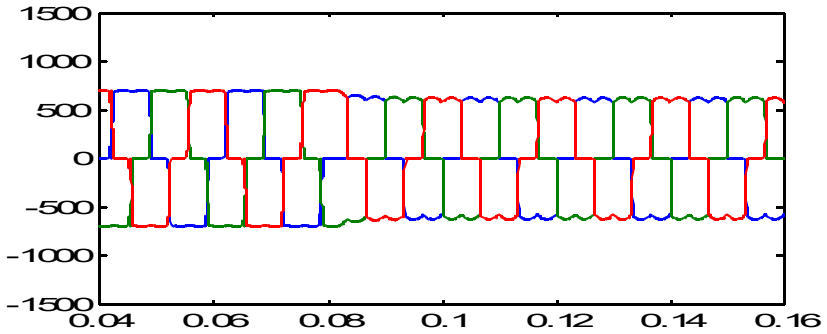

Fig. 17. Load currents before filtering.

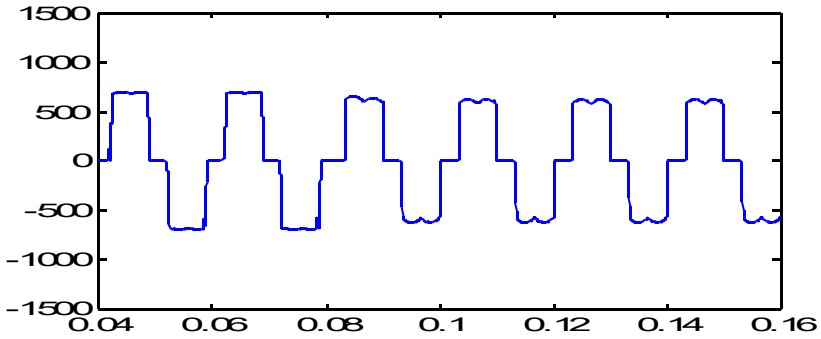

Fig. 18. Load current of phase 1 before filtering.

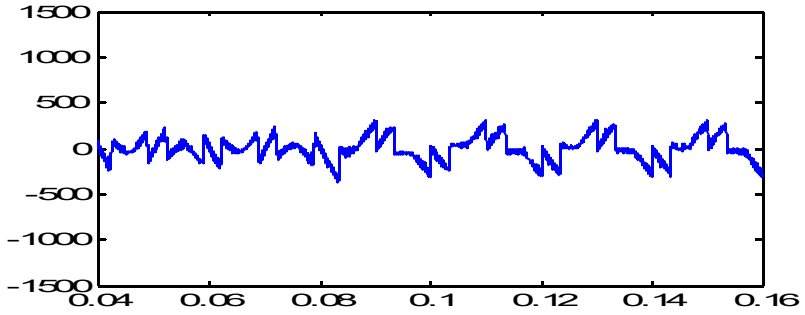

Fig. 19. Harmonic currents injected by inverter A for phase 1.

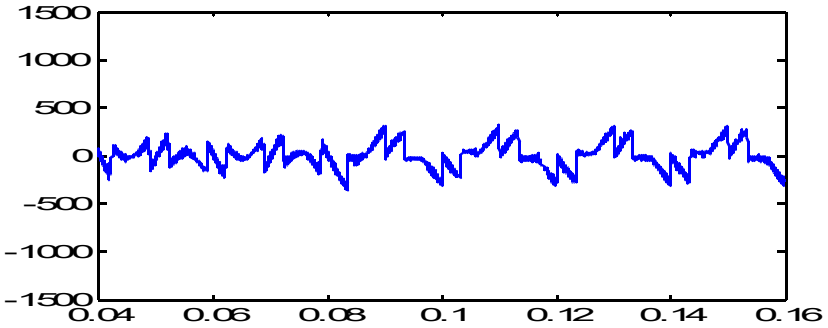

Fig. 20. Harmonic currents injected by inverter B for phase 1.

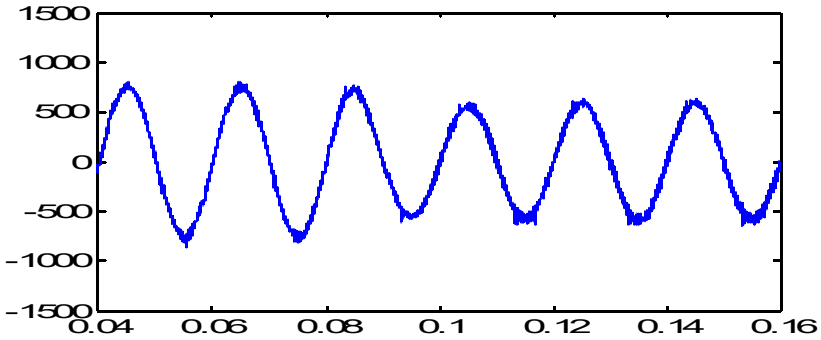

Fig. 21.First phase of the supply current after filtering.

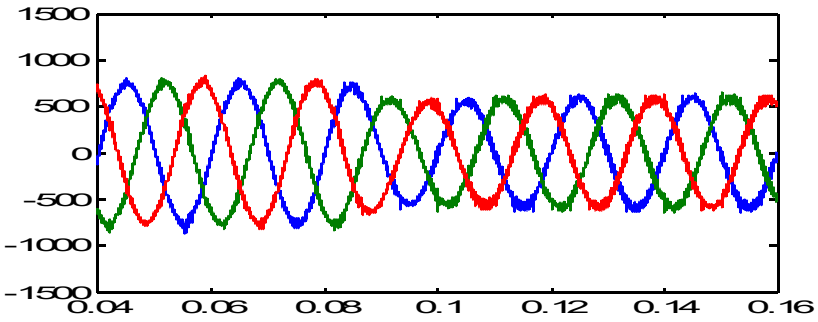

Fig. 22.Supply currents after filtering.

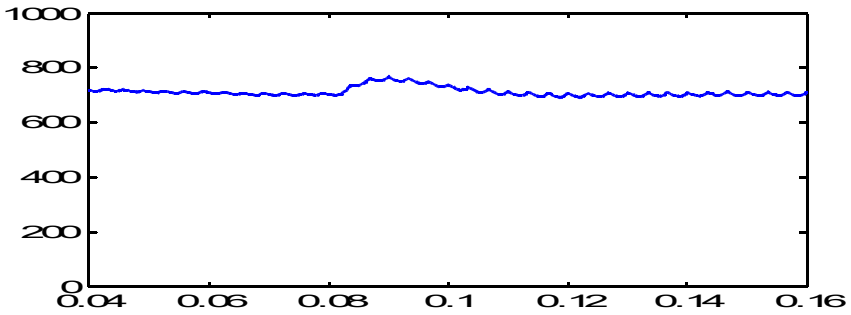

Fig. 23. DC voltage of the modular active power filter.

The THD before filtering for each phase of the electrical network when supplying the three-phase thyristor rectifier is given table 2.

	0°	30° at 0.08 [sec]
Phase 1	26,36%	29,43%
Phase 2	26,98%	29,45%
Phase 3	26,42%	29,50%

Table 2 The THD after filtering becomes for each phase :

	0°	30° at 0.08 [sec]
Phase 1	2,38%	3,01%
Phase 2	2,33%	3,79%
Phase 3	2,36%	3,22%

Table 3

After filtering, we obtain a THD far lower than 5%.

7.Conclusion

In this paper, a modular APF with optimal associated control for zero-sequence current suppression is proposed. The APF studied is based on two inverters. A new PWM control of the two inverters is presented, based on averaged modelling of the APF. Parallel operation for APF in high power level case and zero-sequence current suppression are validated by simulation. Consequently, the method presents an efficient solution for eliminating circulating current in parallel operation. We noted that this condition must be verified to ensure high quality and high performances power filtering.

This approach, based on averaged modelling, and the proposed control concept can be generalized for any modular APF based on N parallel inverters. In this case, harmonic currents references must be the same for each of the N inverters (by division by N the total harmonic currents references) and only one PWM triangular signal must be used.

Appendix A. Simulated system parameters

Source:
V = 240 V
r_s = 1,59 mΩ
l_s = 45,56 µH

RL load:
r_c = 2,73 mΩ
l_c = 23,19 µH
R_{dL} = 0,788 Ω
L_{dL} = 2,6 mH

Modular active power filter constitute by two inverters

inverter A
R_{f1} = 5 mΩ
L_{f1} = 100 µH

inverter B
R_{f2} = 5 mΩ
L_{f2} = 100 µH

V_{dc} = 700 V

PI for dc voltage regulator
$K_c = 2{,}86$
$\tau_c = 2{,}36$ ms

Hysteresis bande
$\Delta I = 50$ A

References

[1] H. Akagi, Y. Kanazawa, A. Nabae, Generalized theory of the instantaneous reactive power filter, Proceeding International power electronics conference. Tokyo, Japan, PP. 1375-1386, 1983.

[2] M. C. Benhabib and S. Saadate, New control approach for four-wire active power filter based on the use of synchronous reference frame, Electric Power Systems Research (Elsevier), vol. 73, Issue 3, pp.353-362, March 2005.

[3] M.C.Benhabib and S. Saadate, A robust control for a shunt active power filter, CIGRE Symposia, Athens, Greece, 13-18 April, 2005.

[4] H. Kevork, J. Geza, Three-phase active filter topology based on a reduced switch count voltage source inverter, 30th Annual IEEE Power Electronics Specialists Conference, Vol. 1, pp. 236-241, June 1999.

[5] H. Kim, F. Blaabjerg, B. Bak-Jensen, J. Choi, Instantaneous power compensation in three-phase systems by using p-q-r theory, IEEE 32nd Annual Power Electronics Specialists Conference , PESC'01 , Vol. 2 , pp. 478 -485, 2001.

[6] A. Campos, G. Joos, P. Ziogas, j. Lindsay, Analysis and design of a series voltage compensator for three-phases unbalanced sources IEEE Transactions on industrial electronics, vol. 39, N° 2, 1992, pp. 159-167.

[7] Ye Zhihong, D. Boroyevich, Jae-Young Choi, F.C Lee, Control of circulating current in two parallel three-phase boost rectifiers, IEEE Transactions on Power Electronics
Volume 17, Issue 5, Sept. 2002, pp. 609 - 615 .

[8] Ye Zhihong, D. Boroyevich, A novel modeling and control approach for parallel three-phase buck rectifiers, IEEE Industry Applications Conference, 2001. Thirty-Sixth IAS Annual Meeting, Vol. 1, 30 Sept.-4 Oct. 2001, pp. 350 –

356.
[9] Ye Zhihong, D. Boroyevich, Fred C. Lee, Paralleling non-isolated multi-phase PWM convertes, IEEE International conference on Industry Applications, Vol. 4, 8-12 Oct. 2000, pp. 2433-2439.

[10] H. Akagi, Y. Tsukamoto, A. Nabae, Analysis and design of an active power filter using quad-series voltage source PWM converters, IEEE Transactions on Industry Applications, Vol. 26, Issue 1, 1990, pp. 93-98.

[11] H. Fujita, S. Tominaga, H. Akagi, Analysis and design of a DC voltage-controlled static VAr compensator using quad-series voltage-source inverters, IEEE Transactions on Industry Applications, Vol. 32, Issue 4, 1996, pp. 970 - 978.

[12] S. Hiti, D. Boroyevich, C. Cuadros, Small-signal Modeling and Control of Three-phase PWM Converters, IAS '94 – IEEE Ind. Appl. Soc. Ann. Meet., pp. 1143-1150, Oct. 1994.

[13] S. Bhattacharya, D. M. Divan, B. Banerjee, Synchronous frame harmonic isolator using active series filter, EPE'91, pp. 3.030-3.35, 1991.

[14] M. C. Benhabib and S. Saadate, A new robust experimentally validated phase locked loop for power electronic control, EPE journal, Vol.15, N°3, 2005.